Long-term Stable and Catalytical 2D MXene nanosheets Wrapped with Aldehyde Xylan for Ultrafast Gelation

Nan Li [a, b‡], Lupeng Shao[c‡], Qiang Xia[a], Shujun Tan[a], Shuwen Zhao[a], XuPeng Li[a], Zhenhua Su [c] Xiang Hao[a, c*], Feng Peng [a, b*]

[a] *Beijing Key Laboratory of Lignocellulosic Chemistry, MOE Engineering Research Center of Forestry Biomass Materials and Energy, Beijing Forestry University, Beijing100083, China*

[b] *China National Pulp and Paper Research Institute, Beijing 100102, China*

[c] *Key Laboratory of Pulp and Paper Science & Technology of Ministry of Education, Qilu University of Technology (Shandong Academy of Sciences), Jinan 250353, China*

*Corresponding Author Email: xianghao@bjfu.edu.cn (Xiang Hao), fengpeng@bjfu.edu.cn (Peng Feng).

Supporting Information

Due to the rigidity of xylan's sugar ring and the fact that the crystalline region can be formed between the hydroxyl groups on the molecular chain by hydrogen bonding, it makes xylan difficult to dissolve in water and more difficult for the preparation of subsequent materials. Therefore, this experiment firstly used sodium periodate ($NaIO_4$) to oxidize xylan to improve the solubility of xylan. As shown in Fig. S1, sodium periodate was able to cause the breakage of C-2 and C-3 bonds in the xylan furan ring during the oxidation process, and the DAX obtained after oxidation was able to dissolve completely in water. Apparently, the unmodified xylan was almost insoluble in the reaction system. The characteristic peak at 1732 cm^{-1} can be seen in the IR spectrum corresponding to the C=O stretching vibration in the aldehyde group. The characteristic peak at 868 cm^{-1} is attributed to the hemiacetal group generated during the oxidation reaction (Fig. S1). In addition, the characteristic structure of DAX can be further confirmed by nuclear magnetic resonance carbon spectroscopy (^{13}C NMR). As shown in Fig. S3, the peaks appeared in C-2 (δ: 91.4 ppm) and C-3 (δ: 86.8 ppm) corresponded to the breakage of C-2, C-3 during the oxidation reaction, which was consistent with the previously reported results. In summary, aldehyde-based xylans (DAX) have been successfully prepared.

Tab. S1. The composition of hydrogels

Samples	AM (g)	KPS (g)	MXene (%)	DAX (%)	CS (%)
MXene $_{1.0}$	0.8	0.008	1	5.0	0
MXene $_{0.5}$	0.8	0.008	0.5	5.0	0
MXene $_{0.1}$	0.8	0.008	0.1	5.0	0
DAX $_{5.0}$	0.8	0.008	1	5.0	0
DAX $_{2.0}$	0.8	0.008	1	2.0	0
DAX $_{1.0}$	0.8	0.008	1	1.0	0
CS $_{2.0}$	0.8	0.008	1	5.0	2.0
CS $_{1.0}$	0.8	0.008	1	5.0	1.0
CS $_{0.5}$	0.8	0.008	1	5.0	0.5

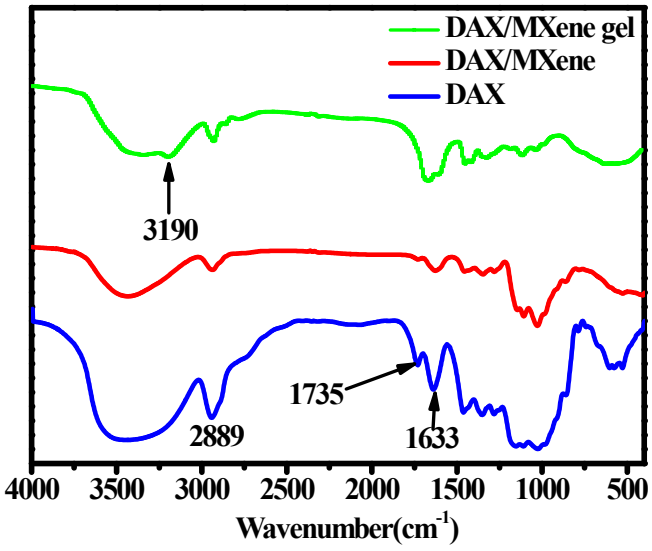

Fig. S1 FT-TR spectra of MXene, DAX, and the MXene-DAX gel.

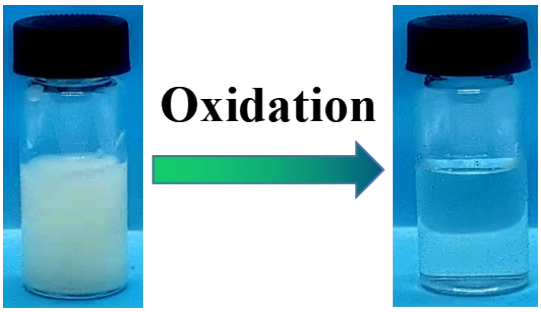

Fig. S2 Xylan was completely dissolved after oxidation.

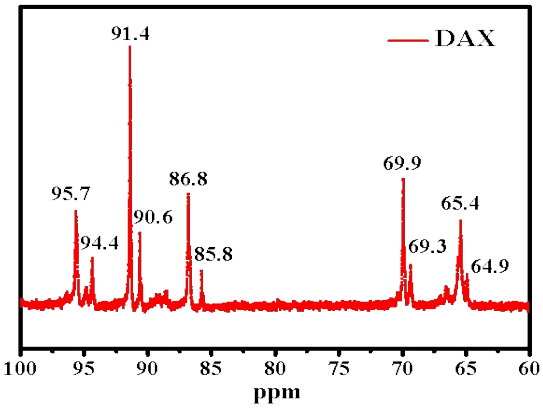

Fig. S3 ^{13}C NMR spectra of DAX.

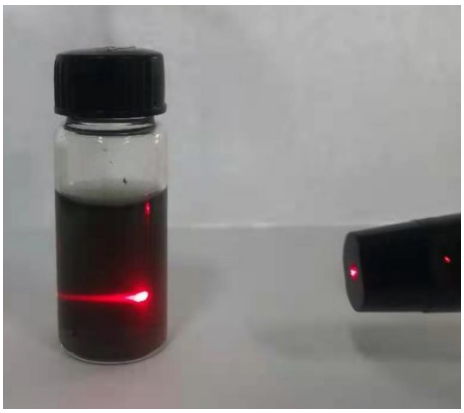

Fig. S4 $MXene_{1.0}$ colloids with the Tyndall effect.

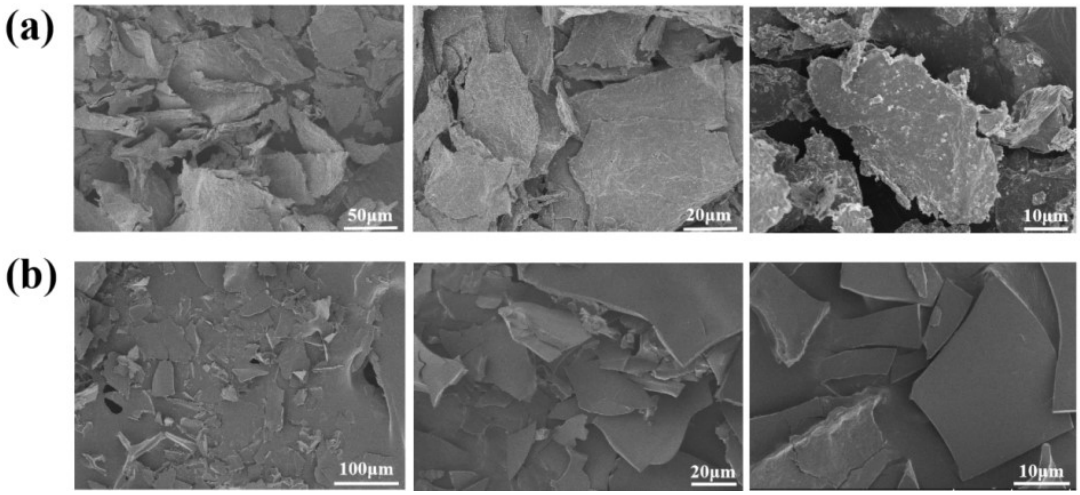

Fig. S5 SEM images of MXene and DAX/MXene, respectively.

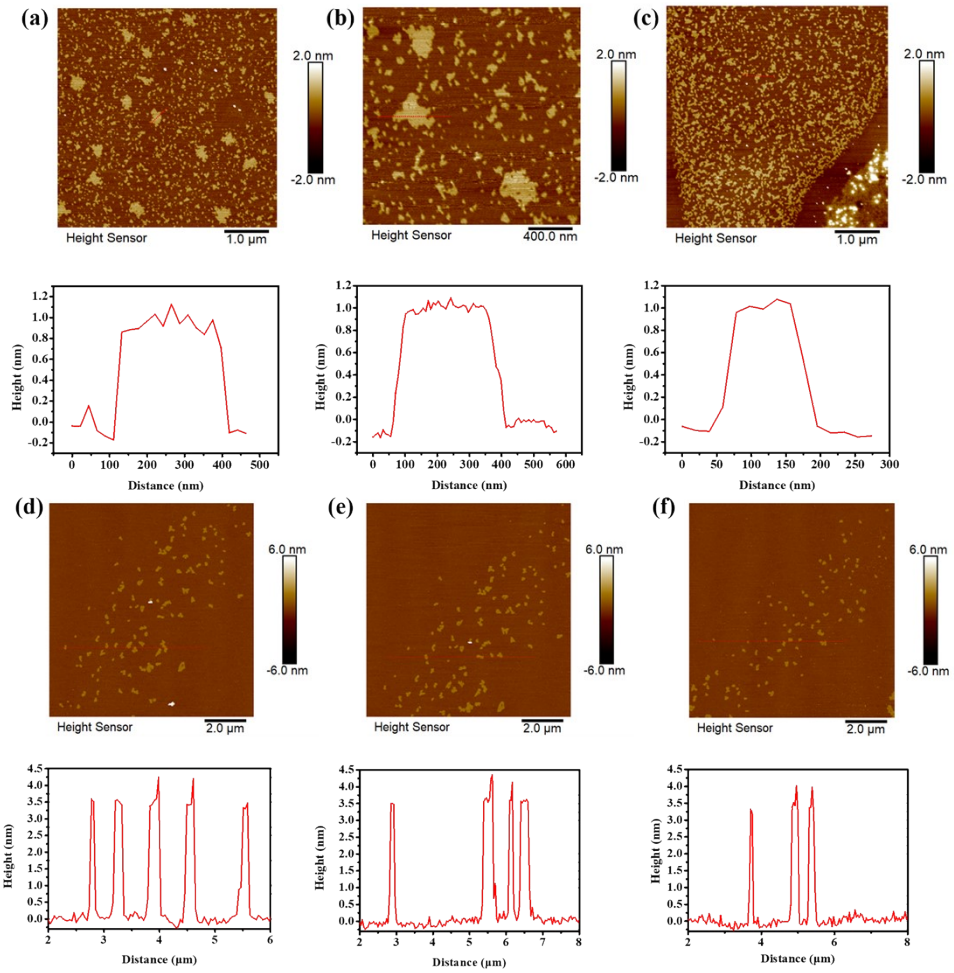

Fig. S6 AFM data of (a-c) MXene alone and (d-f) DAX/MXene mixture.

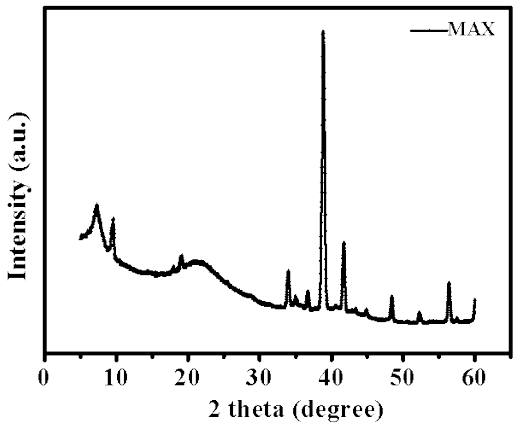

Fig. S7 XRD spectra of MAX.

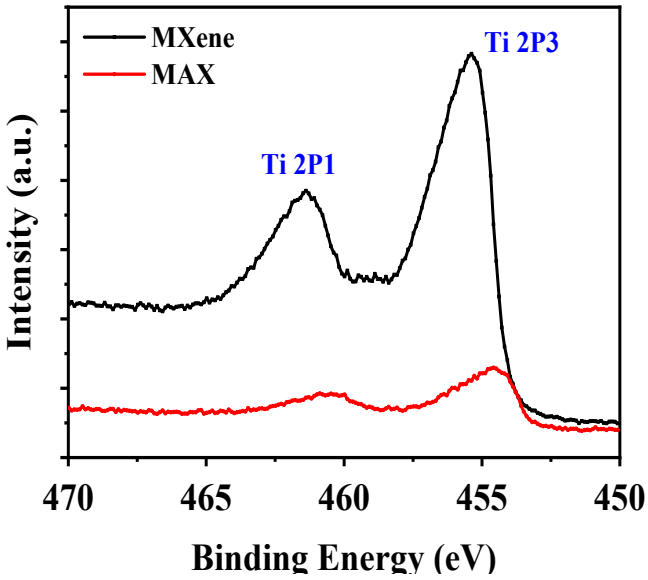

Fig. S8 High-resolution XPS spectra MXene and MAX.

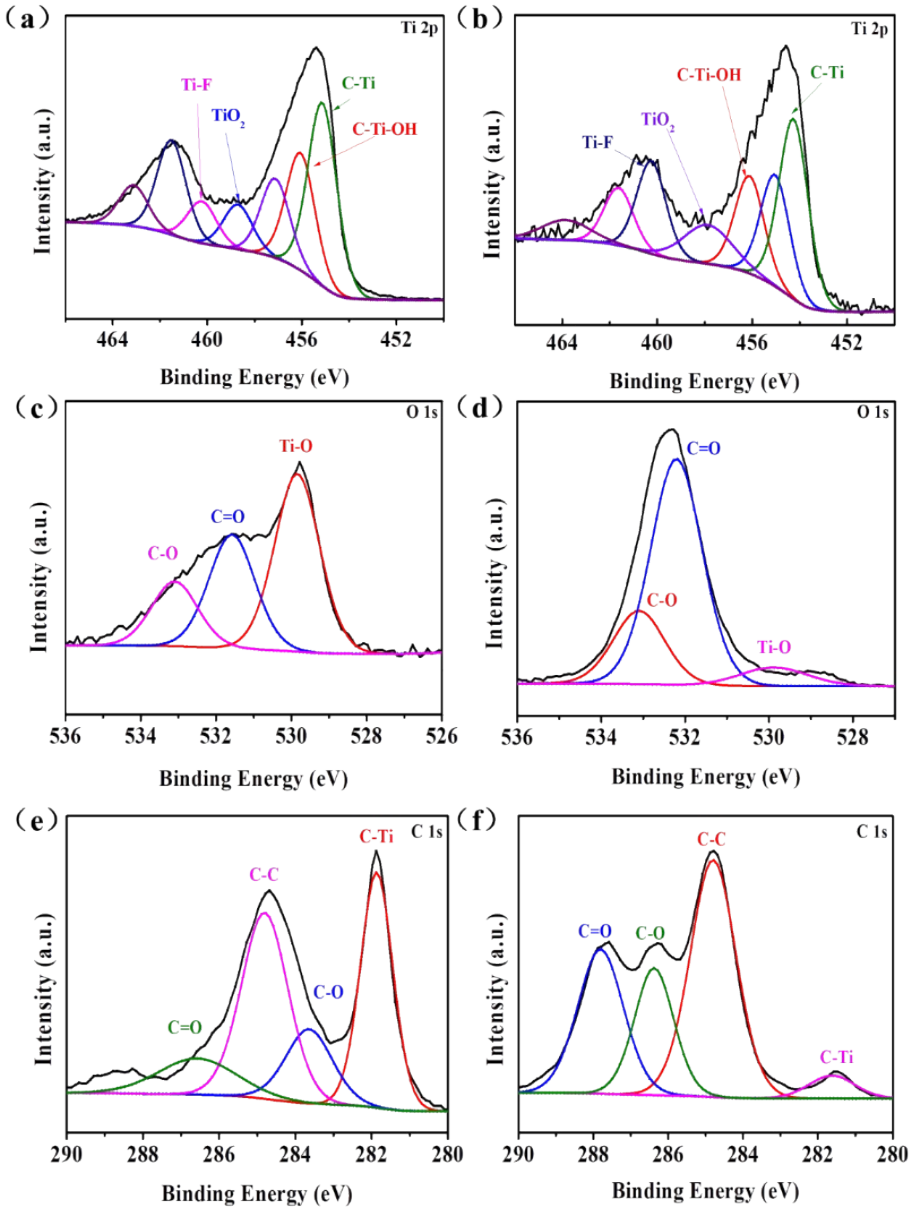

Fig. S9 High-resolution XPS spectra (a)Ti 2p region of (b) O 1s (c) C 1s MXene/DAX mixture (left) and MXene (right).

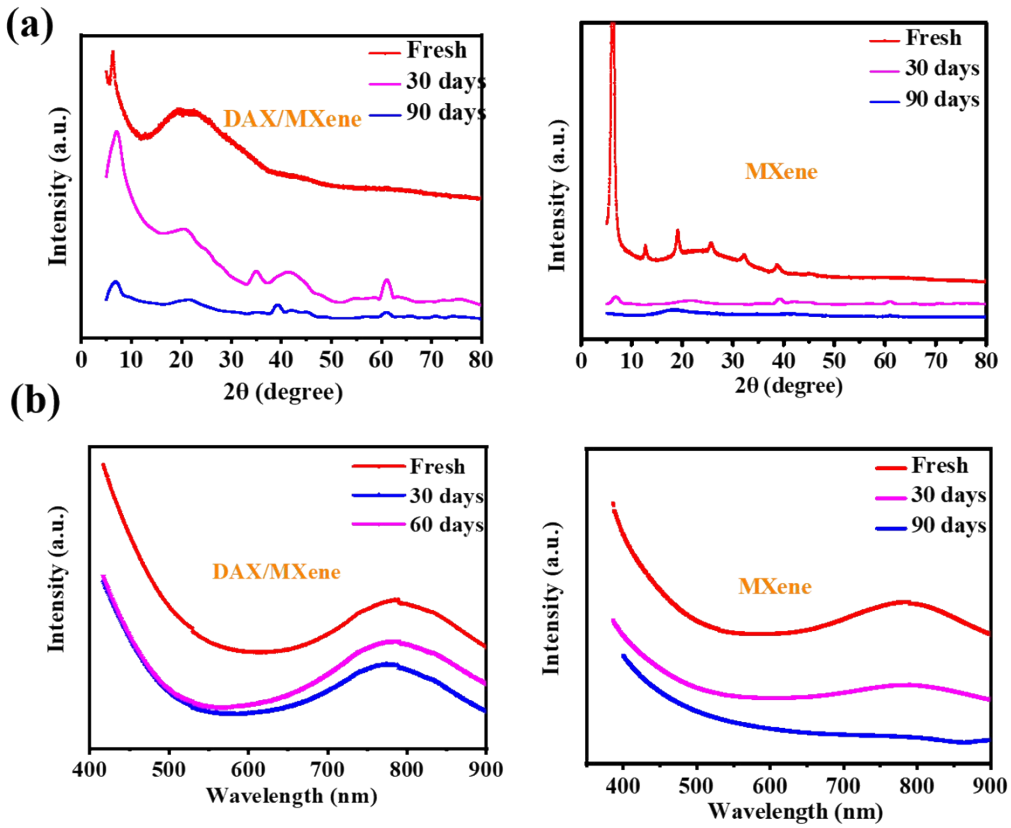

Fig. S10 a) XRD and b) UV-vis spectra of MXene and DAX/MXene, respectively.

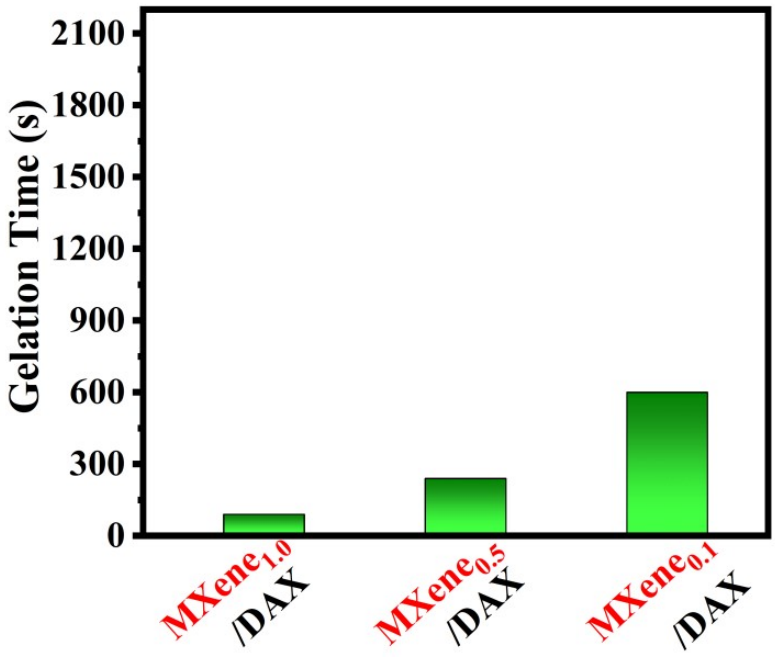

Fig. S11 Gelation time for different MXene concentrations, respectively.

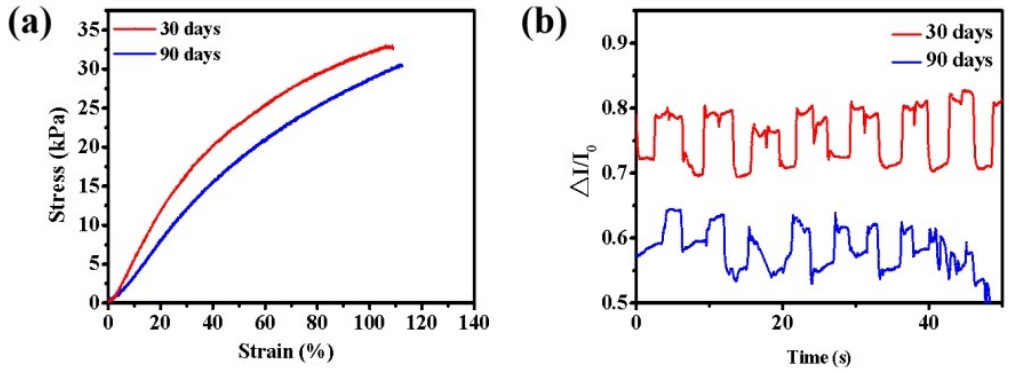

Fig. S12 a) Stress-strain curves of DAX/MXene/PAM hydrogels after different days; b) The signal responses in the form of current changes come from mouth opening/closing, respectively.